Available online at www.eccomasproceedia.org
Eccomas Proceedia COMPDYN (2023) 844-853

ECCOMAS
Proceedia

COMPDYN 2023
9th ECCOMAS Thematic Conference on
Computational Methods in Structural Dynamics and Earthquake Engineering
M. Papadrakakis, M. Fragiadakis (eds.)
Athens, Greece, 12-14 June 2023

NUMERICAL DYNAMIC ANALYSIS OF A MASONRY TRIUMPHAL ARCH: COMPARISON OF DIFFERENT STRENGTHENING CONFIGURATIONS

V. Cardinali[1], B. Pintucchi[2], M. Tanganelli[1], and F. Trovatelli[1]

[1] University of Florence, Department of Architecture
Piazza Brunelleschi n. 6, 50121, Florence, Italy
e-mail: vieri.cardinali@unifi.it, marco.tanganelli@unifi.it, francesco.trovatelli@unifi.it

[2] University of Florence, Department of Civil and Environmental Engineering
Via di Santa Marta n. 3, Florence 50139, Italy
e-mail: barbara.pintucchi@unifi.it

Abstract

Although masonry arches and vaults are often repaired and strengthened with fiber composite materials, there is still a relatively small number of experimental and numerical studies aimed at investigating their dynamic response. This topic is of great interest, especially for some types of structures, such as the triumphal arches and slender barrel vaults found in many Italian churches, that have been proved to be highly vulnerable to seismic actions. Observations of the damages occurred during recent earthquakes have revealed that failure mechanisms were very often activated in triumphal arches, nearly always ending in significant damage, thus requiring repair interventions. With the aim of contributing to this end, numerical dynamic analyses of a masonry triumphal arch of a medium-sized church have been performed and reported in this paper. The reference structure is the masonry triumphal arch built in 2004 at the ELSA Laboratory, where a dynamic identification campaign was carried out to study its in-plane behavior. In this work, a finite-element model of the specimen has been realized for the numerical simulations. Then, an input ground motion has been applied to such structure, and various strengthening configurations hypothesized. From the results obtained, some design indications on the most effective solutions for the improvement of the structure seismic performance are suggested.

Keywords: triumphal arch, nonlinear dynamic analysis, strengthening configuration, strengthening design, seismic assessment

ISSN:2623-3347
Peer-review under responsibility of the organizing committee of COMPDYN 2023.
doi: 10.7712/120123.10439.20817

1 INTRODUCTION

Existing masonry structures have historically exhibited low capacities during seismic ground motions [1-3]. The evidence of post-earthquake damages in many different contexts all over the world have shown that masonry buildings are particularly vulnerable to horizontal actions, especially when orthogonal connections and rigid diaphragms are lacking. In this context, monumental structures require special attention, due to scale effects and the frequent absence of transversal elements. Arched and vaulted structures, given their configurations based on static equilibriums have shown low capacities rapidly leading to higher level of damage [4-5]. For this reason, many researchers were focused on determining compatible and effective strengthening solutions for: i) vulnerability mitigation (as a prevention measure); ii) structural reparation (after the occurrence of a ground motion). Between the different available solutions, fiber reinforcements have increasingly taken field in the restoration interventions [6-8]. These applications can be realized through inorganic matrices compatible with the lime mortar of historical constructions. In addition, they do not alter the general stiffness of the structural system, increasing only the ductility of the configurations.

In historical monuments such as churches and basilica-building typologies, during the seismic motions the structures do not exhibit uniform behaviors, as they point out independent trends based on the performance of each structural macro-element composing the system [9]. Hence, macro-elements (such as the façade, the transept, or the triumphal arches) can be studied separately. In this paper, a comparison of different strengthening solutions based on the application of fiber reinforcements is conducted by numerical simulations. The analysis is performed by considering an independent arch based on laboratory test. The outcomes of the different interventions indicate the most reliable solutions for what concerns the placement of the reinforcement, providing useful indications to set pondered actions on monumental structures.

2 THE CASE STUDY

The case study assumed for the following numerical investigation is a triumphal arch constructed in the ELSA Laboratory and published by [10]. The sample is an independent arch made of brick clay elements and lime mortar. The dimensions of the specimen were chosen on the basis of a study conducted by the same authors investigating the proportions of a family of around 3000 churches surveyed after the 1997 Umbria-Marche earthquake in Italy. The triumphal arch has a height of 5.80 meters, and a 3 m wide opening closed with a round arch (radius of 1.50 meters). The thickness of the piers is 95 cm, with a depth of 60 cm. The two piers were placed over two different supports, a movable one made by steel on the left side and a reinforced concrete basement on the right side. The authors provided a dynamic monitoring of the specimen; the results have pointed out two in plane natural frequencies at 8.65 and 46.05 Hz respectively. In the central part of the arch, a double peak around 28 Hz was found (27.40 and 28.30 Hz).

In this work, the specimen has been selected to investigate the structural performance of different strengthening configurations.

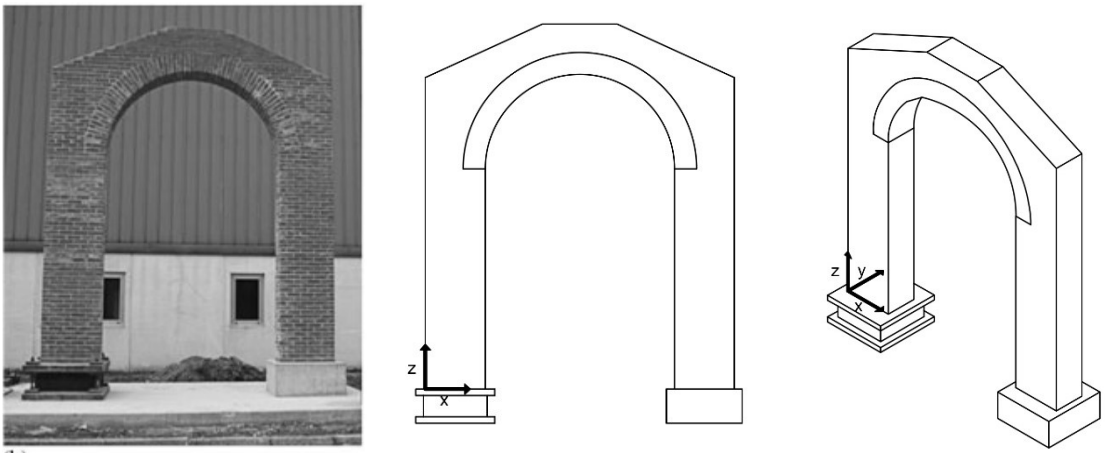

Figure 1: The experimental case study, adapted from [10].

2.1 Numerical modeling and calibration

The numerical modeling was executed on the FE environment Abaqus CAE [11]. A 3D CAD model was imported using the iges format and meshed in Abaqus for the numerical simulations. In this work, a homogenous macro-modeling approach has been used, and masonry represented as a continuum material. The FE model consists of 69324 hexahedral elements (C3D8), 78936 nodes and 236808 degrees of freedom. A linear modal analysis was conducted assuming the following mechanical parameters: an Elastic Young's Modulus equal to 2000 MPa, a Poisson's ratio ν of 0.20 and a density of 1800 kg/m^3. The analysis leads to a fundamental frequency (in plane) of 7.21 Hz; although the result has a lower value compared to the experimental one, this was due to the use of more precautionary mechanical parameters, which were considered more appropriate for the aims of the study.

The seismic performance of the masonry structure has been determined considering the non-linear capacity of masonry. The constitutive law of the masonry was characterized through the Concrete Damage Plasticity model (CDP) [12]. Although it has been conceived for homogenous materials such as the concrete, several applications at different scales have proved its reliability for masonry buildings and vaulted structures [13-16].

The CDP model is characterized by an isotropic material with a plasticity-damage relation. Different parameters rule its plasticity, influencing the non-linear response. Within them, the dilatation angle Ψ, the flow potential eccentricity e, the ratio K_c, the ratio between the initial biaxial compressive yield stress and the uniaxial stress f_{b0}/f_{c0}, the viscosity μ. The values adopted for each parameter, determined in accordance with the literature [17], are shown in Table 1. Regarding the resistance parameters, in absence of specific investigations, the values suggested by [18] have been adopted. Since this is a good quality masonry the compressive strength f_c has been assumed according to the maximum value of the range available for clay brick masonry with lime mortar and equal to 4.3 MPa. Hence, the tensile strength of the masonry f_t has been assumed as the 5% of the compressive one and equal to 0.21 MPa.

The tensile softening has been described by the fracture energy G_{ft} through a stress-displacement relation [19]. G_{ft} has been computed according to [20] through the relationship $G_{ft} = 0.025(2f_t)^{0.7}$ obtaining a value of 13.62 N/m. Compression softening is described by a stress/strain ratio; however, in the following phases of analyses, no significant compression collapses have been detected.

Damage parameter (d_c and d_t) follow a linear law where the 90% of damage is set as the ultimate condition, as shown in (Tab. 2).

Ψ	e	fb0/fc0	Kc	μ
Dilation angle	Eccentricity	Biaxial strength ratio	Drucker-Prager correction parameter	Viscosity parameter
10°	0.10	1.16	0.667	0.0001

Table 1: CDP general parameters adopted in the analyses.

Compression		Tension	
dc [-]	Anelastic strain [-]	dt [-]	Displ. [mm]
0	0	0	0
0.9	0.016	0.9	0.2

Table 2: parameters adopted for the damage evolution in the model.

2.2 Numerical dynamic analyses

Nonlinear dynamic analyses of the case study have been performed by using acceleration recorded during the Aquila earthquake (6th April 2009 – AQA-V. Aterno- F. Aterno), as seismic input motion. In the numerical analysis, damping was assumed through the Rayleigh model, where the required coefficients α and β were calculated with reference to the first two natural frequencies and assuming a damping coefficient of 2%. The input ground motion was applied at the base of the model, which was assumed fixed through constraints. In the elevation, all the nodes of the model have been fixed in the plane *xz* (Fig. 1), while the accelerogram has solely be applied in the x direction. Three distinct control points have been accounted, one in a central position over the keystone of the arch (PC), and two lateral control points located on the external piers of the structure (PCL and PCR for left and right element respectively). The results of the analysis are presented in terms of tensile damage and time history of the top displacement. The arch shows a classic macro-element behavior with an alternate formation of the hinges between the intrados and extrados (Fig. 2). The rotations of the system involve the whole structure, with the formation of two fractures at the basement of the piers. These represent the first cracks that appeared in the model. Hence, the left fracture starting from the intrados (hinge at the extrados) occurred, followed by the one on the other side at the extrados. The top hinges are located around at 45 degrees, with a minor opening located at the horizontal connection between the right pier and the arch. In terms of displacements, the control points located at the top of the system show that the fractures occur at around 2.47 s, then the three points show a residual displacement which is given by the opening fracture of the model. The maximum residual displacement is expressed by PCR point, with a value of 10.7mm; PCL presents a residual of 2.6 mm while the central PC a displacement of 6.8 mm.

3 EVALUATION OF VARIOUS STRENGTHENING CONFIGURATIONS

On the basis of the above-described performances of the triumphal arch under the applied seismic input, different fiber reinforcements have been considered. The various strengthening configurations are realized with the same reinforcement but different placements, in order to comparatively evaluate their effectiveness. It is worth noting that in the strengthening design of masonry structures different issues should be considered. Especially in monumental structures, such as churches and basilicas, any interventions and their possible applications should be evaluated also in relation to their compatibility with existing decorative elements, such as frescoes, etc.

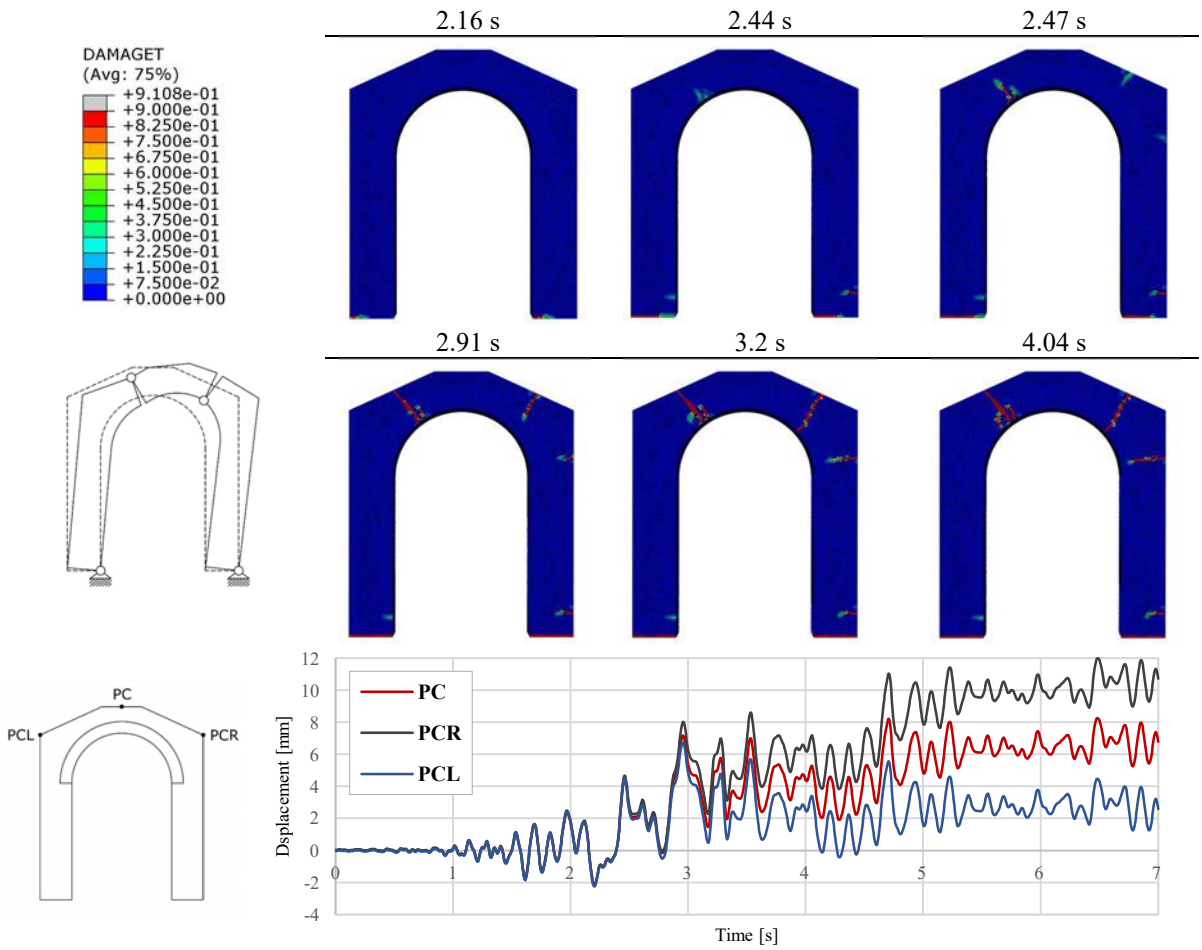

Figure 2: Above: damage crack pattern and kinematic failure mechanism of the triumphal arch; below: time-history of horizontal displacement at the three considered control points.

As fiber reinforcement, Kerakoll Geosteel G1200 has been chosen (Tab. 3). It is realized through a unidirectional galvanized steel fiber sheet, made of steel micro-cords, and fixed to a fiberglass micromesh. The reinforcement is particularly suitable for masonry structures as it can be combined with mineral matrixes compatible with the existing supports. In this work, four different strengthening configurations have been adopted, by placing the reinforcement in various layouts as shown in Fig. 3. Internal and only applied to the intrados of the arch (I), internal and involving the arch + the piers (IP), at the extrados of the triumphal arch (E), at the extrados yet involving the piers (EP).

Kerakoll G1200	
Conventional tension limit	839 MPa
Conventional deformation limit	0.43%
Elastic modulus of the sheet	195 MPa
Mortar compressive resistance class (typical value)	>15 MPa (28 days)

Table 3: mechanical properties of the Kerakoll G1200 reinforcement.

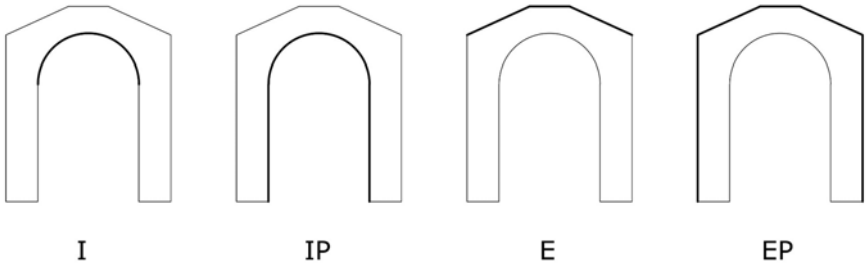

Figure 3: the analyzed strengthening configurations.

In the numerical model, the reinforcement has been realized through a 4-node doubly curved thin shell elements (S4). A linear elastic behavior has been adopted for the fiber, and debonding phenomena have not been accounted for. The strengthening has been modeled considering an equivalent thickness of the material equal to 0.169 mm, with an Elastic Young's Modulus of 195 GPa and a Poisson's ratio ν of 0.35. In all the models used, the reinforcement has been applied over the whole thickness of the triumphal arch. The four different configurations have been compared in terms of time-history displacement, crack pattern and residual deformation. Fig. 4 shows drawings of the different crack patterns.

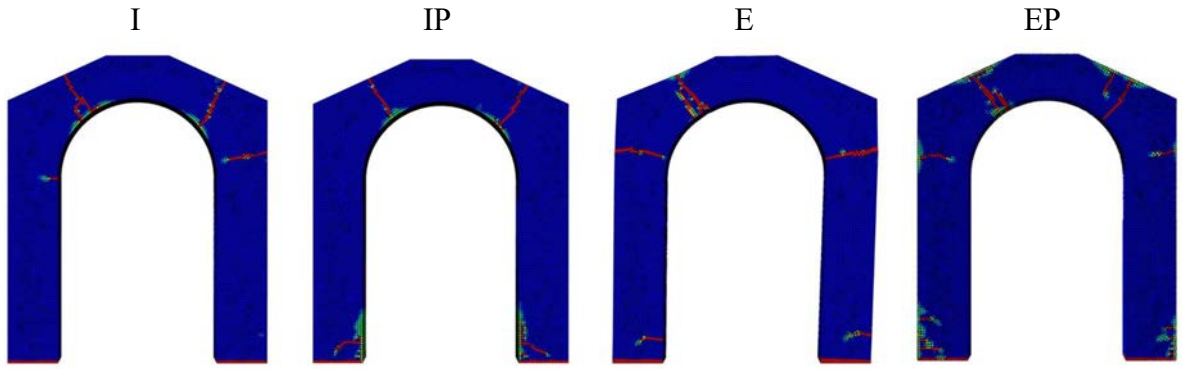

Figure 4: Tensile damage (same color scale as figure 2) crack patterns for different strengthening configurations.

The comparison between the cases considered has also been conducted in terms of horizontal relative displacement for the three control points (Fig. 5). In addition, for the PCR control point a further comparison in terms of base shear and displacement is shown (Fig. 5).
Overall, the analyses evidence similar results for the I, IP, and EP models. The IP and EP models exhibit the best performances, by limiting the top displacement of the nodes. For what concerns the external reinforcement E, the solution does not provide adequate strengthening improvements. This is visible for all the control points, and especially for PCL, where the residuals in the strengthened arch reach higher amplitudes than those of the unreinforced one. Observing the damage patterns, models IP and EP exhibit patterns similar to each other, which are justifiable by excluding the debonding effects on the fiber reinforcement. The improvement at the intrados of the arch leads to similar displacement and crack patterns, limiting the structure's deformations.

Considering the similar outcomes of the three above-mentioned models (I, IP and EP), the one assumed as the most effective one in terms of structural performances, i.e. the external model involving the arch and the piers EP, has been tested considering a ground motion increase at 150% of its intensity. The results have been compared with the unreinforced model tested for the same input ground motion.

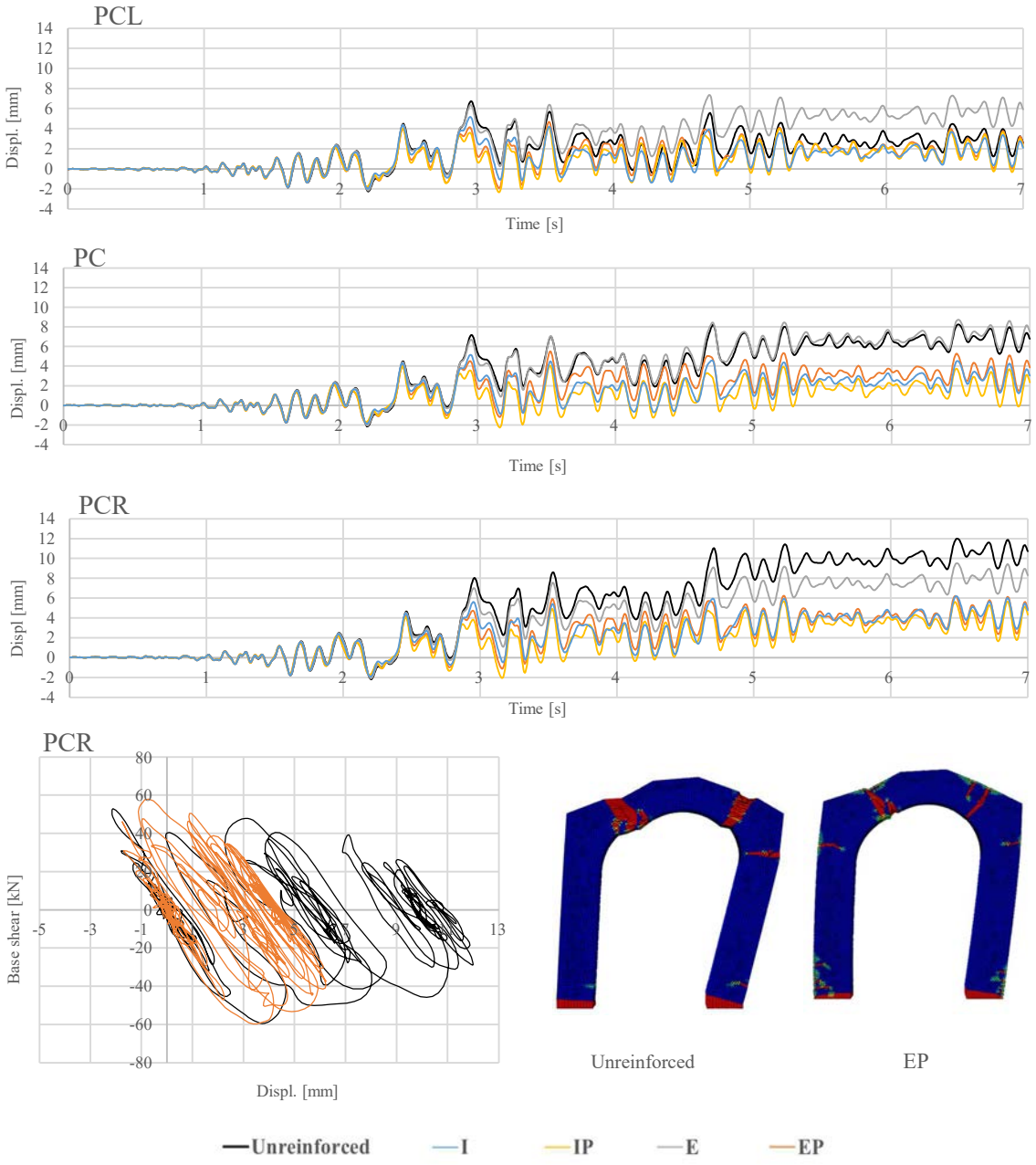

Figure 5: Above: horizontal time history displacements at the three control points; below, on the left: base shear vs displacement at PCR control point for the EP configuration; on the right: deformed configurations of the unreinforced and EP models (scale factor =100).

In Fig. 6, the results are shown in terms of top base shear as a function of displacement and damage crack pattern. The application of an increased seismic motion exhibits the effects of the reinforcements. Fiber reinforcement applied to the piers and arch leads to an effective confinement that limits the crack opening.

The residuals of the three control points do not evidence different values like for the unreinforced case, but the structure is able to guarantee a more homogenous behavior with a minor dimension of the crack width.

For what concerns the damage pattern, the crack patterns of the strengthened solutions (Fig. 6) show a higher damage along the contact surface between the fibers and the solid masonry

elements. This is given by the tangential stress generated by the capacity of the reinforcement overcoming the value of the masonry range. In any case, both the displacements as the crack patterns of the unreinforced configurations show a case where the macro-element tend to behave according to three distinct blocks, with the formation of higher cracks leading to significant damage and potential failure of the system.

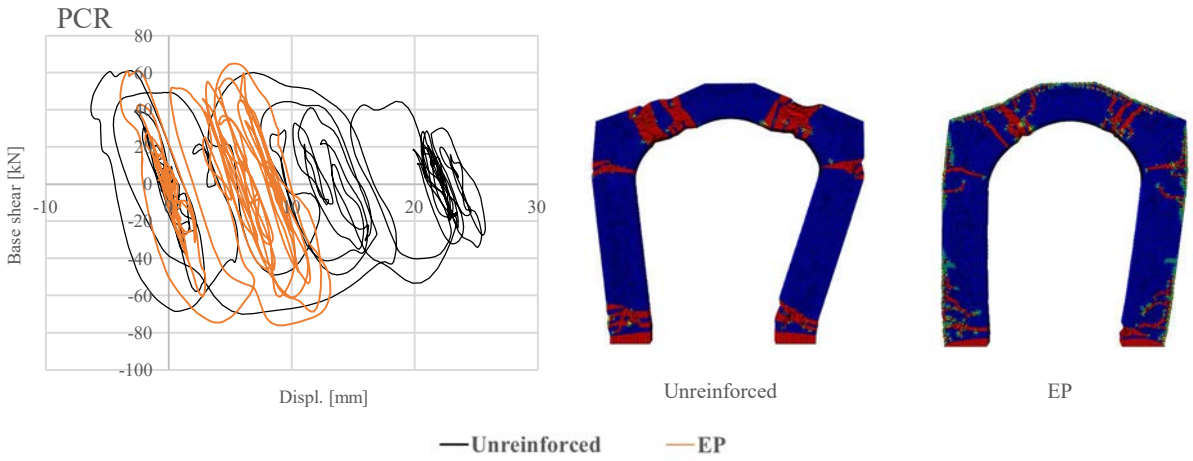

Figure 6: L'Aquila 150% earthquake: comparison between unreinforced and EP strengthened configuration. On the left, base shear vs top displacement for the PCR control point. On the right, comparison in terms of crack pattern and deformed configuration (def. scale factor =100).

4 CONCLUSIONS

In this paper a numerical comparison of different strengthening solutions for a triumphal masonry arch is proposed. The model has been realized on the basis of the specimen made in the ELSA Laboratory and published by [10]. The structural performances of the macro-element have been evaluated by applying the L'Aquila earthquake record. A finite-element model of the specimen has been realized and calibrated for the seismic assessment, which has been conducted by means of nonlinear dynamic analysis. Various fiber reinforcement strengthening configurations have been considered and numerically evaluated both in terms of top displacement/base shear ratios and of crack pattern. The results show that the placement of the reinforcement at the extrados of the triumphal arch is the solution providing the poorer improvements. Conversely, the other solutions revealed compatible seismic retrofitting. Further studies are needed, in order to parametrize the structural response by varying different features, accounting also for different seismic inputs with different frequency contents. In addition, the constitutive law of the fiber reinforcements could be further implemented in order to account for the debonding effects and the interactions between fiber reinforcement and supports. Strengthening solutions alternative to the fiber application (e.g. the insertion of tie rods) can be also assessed. Lastly, the assumptions of different architectural ratios in terms of slenderness, height and length of both piers and the arch can be considered in order to parametrize the structural response of the triumphal arches, providing insights on their vulnerability and for strengthening solutions.

REFERENCES

[1] S. Taffarel, M. Giaretton, F. Da Porto, C. Modena, C., *Damage and vulnerability assessment of URM buildings after the 2012 Northern Italy earthquakes*. In: Brick and Block

Masonry - Trends, Innovations and Challenges, 16th International Brick and Block Masonry Conference Padova, Italy, 26-30 June, 2016

[2] N. Augenti, F. Parisi, *Learning from construction failures due to the 2009 L'Aquila, Italy, earthquake,* Journal of Performance of Constructed Facilities, 24(6), 536-555, 2010.

[3] A. Penna, P. Morandi, M. Rota, C.F. Manzini, F. Da Porto, G. Magenes, *Performance of masonry buildings during the Emilia 2012 earthquake.* Bull Earthquake Eng 12, 2014, 2255–2273 https://doi.org/10.1007/s10518-013-9496-6

[4] F. Doglioni, A. Moretti, V. Petrini, *Le chiese e il terremoto*. Edizioni Lint, 1994, Trieste, Italy.

[5] F. Da Porto, B. Silva, C. Costa, C. Modena, *Macro-scale analysis of damage to churches after earthquake in Abruzzo (Italy) on April 6, 2009*. J. Earthq. Eng. 16 (6), 2012, 739-758.

[6] B. Pintucchi, N. Zani, *A simple model for performing nonlinear static and dynamic analyses of unreinforced and FRP-strengthened masonry arches*. European Journal of Mechanics - A/Solids, (), 2016, S0997753816300389–. doi:10.1016/j.euromechsol.2016.03.013

[7] P. Zampieri, N. Simoncello, C.D. Tetougueni, C. Pellegrino, *A review of methods for strengthening of masonry arches with composite materials*. Engineering Structures, 2018, 171(), 154–169. doi:10.1016/j.engstruct.2018.05.070

[8] I. Boem, *Masonry elements strengthened through Textile-Reinforced Mortar: application of detailed level modelling with a free open-source Finite-Element code*, Construction and Building Materials, Volume 357, 2022, 129333, ISSN 0950-0618,

[9] E. Cescatti, S. Taffarel, A. Leggio, F. Da Porto, C. Modena, *Macroscale damage assessment of URM churches after the 2016 earthquake sequence in Centre of Italy*, Convegno ANIDIS. L'ingegneria sismica in Italia ANIDIS XVII, 2017, Pistoia, 17 2 21 settembre.

[10] S. Podestà; G. Riotto; F. Marazzi, *Reliability of dynamic identification techniques connected to structural monitoring of monumental buildings*. 2008, 15(4), 622–641. doi:10.1002/stc.219

[11] ABAQUS, *Theory and user's manuals 2018*. Pawtucket (RI, USA): Hibbit, 2018, Karlsson and Sorensen.

[12] J. Lubliner, J. Oliver, S. Oller, E. Oñate, *A plastic-damage model for concrete*. Int J Solids Struct 1989. doi:10.1016/0020-7683(89)90050-4.

[13] S. Degli Abbati, A.M. D'Altri, D. Ottonelli, G. Castellazzi, S. Cattari,S. De Miranda, S. Lagomarsino, *Seismic assessment of interacting structural units in complex historic masonry constructions by nonlinear static analyses*. Computers & Structures, 2018, (), S0045794918306916–. doi:10.1016/j.compstruc.2018.12.001

[14] G. Milani, M. Valente, M. Fagone, T. Rotunno, C. Alessandri, *Advanced non-linear numerical modeling of masonry groin vaults of major historical importance: St John Hospital case study in Jerusalem*. ENGINEERING STRUCTURES, vol. 194, pp. 458-476, 2019

[15] V. Cardinali, B. Pintucchi, M. Tanganelli, F. Trovatelli, *Settlement of masonry barrel vaults: an experimental and numerical study*, Procedia Structural Integrity Volume 44, 2023, Pages 1252-1259

[16] Cardinali V., Tanganelli M., Trovatelli F., Finite-element seismic assessment of a masonry cross vault through blind predictions and numerical simulations, International Journal of Architectural Heritage, submission ongoing.

[17] A.M. D'Altri, V. Sarhosis, G. Milani, et al. *Modeling Strategies for the Computational Analysis of Unreinforced Masonry Structures: Review and Classification*. Arch Computat Methods Eng 27, 1153–1185 (2020). https://doi.org/10.1007/s11831-019-09351-x Engineering, 110, 87–101.

[18] MIT, *Circolare 21 gennaio 2019, n. 7 Istruzioni per l'applicazione dell'«Aggiornamento delle "Norme tecniche per le costruzioni"» di cui al decreto ministeriale 17 gennaio 2018*. G.U. n. 47 del 26/02/2009, Supplemento Ordinario n. 27, 2019, Rome, (in Italian)

[19] A. Hillerborg, M. Modéer, P.E. Petersson, *Analysis of crack formation and crack growth in concrete by means of fracture mechanics and finite elements*. Cement and Concrete Research 1976; 6:773–81. doi:10.1016/0008-8846(76)90007-7.

[20] P.B. Lourenço, *Recent advances in masonry modelling: micromodelling and homogenisation*. Multiscale Model. Solid Mech. 2008: 251–94. https://doi.org/10.1142/9781848163089_0006.